The Representation of AC Machine Dynamics by Complex Signal Flow Graphs

Joachim Holtz, *Fellow, IEEE*
University of Wuppertal,
42097 Wuppertal – Germany

Abstract — **Induction motors are modelled by nonlinear higher-order dynamic systems of considerable complexity. The dynamic analysis based on the complex notation exhibits a formal correspondence to the description using matrices of axes-oriented components; yet differences exist. The complex notation appears superior in that it allows to distinguish between the system eigenfrequencies and the angular velocity of a reference frame which serves as the observation platform. The approach leads to the definition of single complex eigenvalues that do not have conjugate values associated to them. The use of complex state variables further permits the visualization of ac machine dynamics by complex signal flow graphs. These simple structures assist to form an understanding of the internal dynamic processes of a machine and their interactions with external controls.**

1. Introduction

The graphic representation of dynamic systems by signal flow graphs is a well established tool in control systems engineering. It is based on the analysis of the system in the time domain which commonly results in a set of first-order differential equations. The cross-coupling between the equations is conventionally represented by signal flow graphs in which the individual differential equations appear as transfer elements. There are only a few types of basic transfer elements required to represent any arbitrary dynamic system. Typical linear transfer elements are integrators, first-order delay elements, second-order delay elements, being classified either as overdamped or underdamped, and time delay elements. Controllers are represented by proportional-integral (PI) elements, proportional differential (PD) elements or the combination of those two, the PID element. Nonlinear system characteristics enter a signal flow graph as specific nonlinear functions, signal multipliers, or signal dividers.

A signal flow graph is a form of graphic notation which contains the same complete information on a dynamic system as the set of differential equations, or as its frequency domain equivalent, the transfer function. Naturally, a signal flow graph will not provide particular solutions that describe the dynamic behavior of a system under the influence of specific external forcing functions. However, a signal flow graph does have the distinct advantage of conveying information on the basic system characteristics in an easy to understand graphic notation. This makes the dynamic performance of a system intelligible just by visual inspection.

AC machines are fairly complex nonlinear systems. This is the reason why the graphic representation by signal flow graphs is not a frequent practice [1], [2]. The result of such representation is indeed a very involved and highly cross-coupled graphical structure [3]. The efforts to extract meaningful information from such graph are little rewarding. Control systems engineers have preferred therefore to study differential equations and transfer functions, instead.

This paper presents an alternative approach for the description of ac drive systems by signal flow graphs. The approach is based on the space vector theory [4].

2. AC Machine Winding

2.1 A single phase winding

Consider an ac machine having only a single phase winding in the stator. The voltage equation of this phase winding is

$$u_{s\alpha} = r_s i_{s\alpha} + \frac{d\psi_{s\alpha}}{d\tau} \tag{1}$$

where $u_{s\alpha}$ is the phase voltage, $i_{s\alpha}$ the phase current, r_s the winding resistance, and

$$\psi_{s\alpha} = l_s i_{s\alpha} + \psi_{rp\alpha} \tag{2}$$

the flux linkage of the winding. The winding inductance is l_s, and the term $\psi_{rp\alpha}$ represents other flux components that are linked with the winding under consideration; they may originate from a permanent magnet rotor, for example. All quantities are normalized with respect to their rated amplitudes. Time is also normalized: $\tau = \omega_{sR} t$, where ω_{sR} is the rated stator frequency.

Note that the scalar terminal voltages and currents in the foregoing equations refer to a lumped parameter equivalent of the machine. The effect of these quantities inside the machine is of different nature. The current produces the machine torque which originates from the sum of tangential forces that are distributed on the stator surface. Neglecting end effects, the force density distribution varies with the respective location along the circular airgap, and hence is a function of space. Although this function depends on the external machine currents, it is not completely defined by their scalar values. The following discussion will make this even more clear.

The current $i_{s\alpha}$ is the winding current that can be measured outside the machine at the winding terminal. Inside

Invited Paper: *IEEE Transactions on Industrial Electronics*, Vol. 42, No. 3, 1995, pp. 263-271.

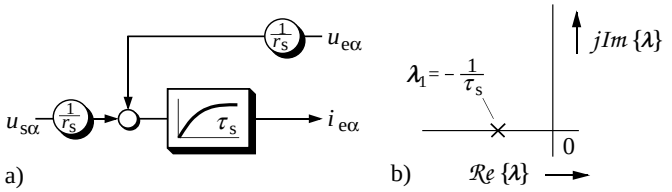

Fig. 1: Dynamic representation of a phase winding, a) signal flow graph, b) root locus showing a single pole

the machine, this current produces a magnetic field component which is assumed to have a sinusoidal distribution around the air-gap, neglecting space harmonics that do not contribute to the average torque. This assumption entails a sinusoidal mmf distribution which can be imagined as the effect of a sinusoidal distribution in space of the winding conductors.

Sinusoidal distributions in space can be mathematically described by space vectors. The space vector $\boldsymbol{i}_{s\alpha}$ in (1) represents the spatial mmf distribution caused by the phase current $i_{s\alpha}$, as the other phase windings are not yet considered. The vector is centered in the origin of the complex plane and has an angular orientation that coincides with the geometrical winding axis, which is the α-axis in this case. The magnitude of the space vector $\boldsymbol{i}_{s\alpha}$ equals the winding current $i_{s\alpha}$.

The voltage $u_{s\alpha}$ across the winding terminals is composed of the resistive drop and the induced voltage, as indicated by (1). Inside the machine, these voltages are sinusoidally distributed. This is due to the sinusoidal distribution of the winding conductors which determines the distributions in space of both the resistive drop and the induced voltage. While the external phase voltage $u_{s\alpha}$ at the machine terminals is a scalar quantity, its spatial distribution inside the machine is described by the voltage space vector $\boldsymbol{u}_{s\alpha}$. The magnitude of the space vector $\boldsymbol{u}_{s\alpha}$ equals the winding voltage $u_{s\alpha}$.

The voltage equation of the phase winding is derived from (1) and (2) as

$$u_{s\alpha} = r_s i_{s\alpha} + l_s \frac{di_{s\alpha}}{d\tau} + u_{e\alpha} \qquad (3)$$

and visualized in the signal flow graph Fig. 1(a). The scalar winding current $i_{s\alpha}$ is chosen as the state variable. The back emf voltage $u_{e\alpha}$ is induced by the revolving rotor field. This voltage is considered independent from the stator current in a first approach; such situation may prevail, for instance, in machines having a permanent magnet rotor. The resulting first-order system is characterized by one real eigenvalue $\lambda_1 = -r_s/l_s = -1/\tau_s$ which is located on the negative real axis of the root locus plot, Fig. 1(b).

2.2 Two axis representation

Consider now a second phase winding in the stator, having its axis, the β-axis according to Fig. 2(a), arranged in quadrature with respect to the α-axis of the first winding. Each of the two external winding currents i_{sa} and i_{sb} produces a sinusoidal mmf wave inside the machine. These

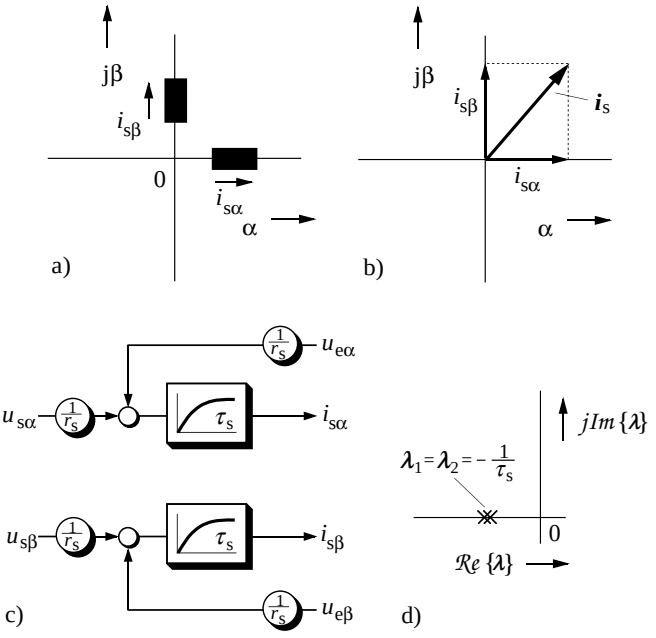

Fig. 2: Two-phase winding in stationary coordinates; a) winding arrangement, b) space vector diagram, c) signal flow diagram of space vector components, d) root locus showing two real poles

distributions are represented by two space vectors in Fig. 2(a), $\boldsymbol{i}_{s\alpha} = i_{s\alpha} \cdot e^{j0}$ and $\boldsymbol{i}_{s\beta} = i_{s\beta} \cdot e^{j\pi/2}$. The magnitudes of these space vectors depend on the respective winding currents, while their phase angles are fixed. They coincide with the directions of the respective winding axes. The total mmf distribution in space may vary in magnitude as well as in phase angle. It is obtained as the superposition of the two sinusoidal components and can be described by the space vector $\boldsymbol{i}_s$ in Fig. 2(b) as the sum of the spatial distributions $\boldsymbol{i}_{s\alpha}$ and $\boldsymbol{i}_{s\beta}$.

Owing to their arrangement in quadrature, there are no common flux linkages between the α- and the β-winding. The air-gap field may nevertheless assume any magnitude and direction in space. It comprises of a component proportional to $\boldsymbol{i}_s$, which in turn depends on the respective values of the phase currents $i_{s\alpha}$ and $i_{s\beta}$. The two phase windings can be consequently considered equivalent to any three-phase or polyphase winding arrangement. This enables to treat the current components $i_{s\alpha}$ and $i_{s\beta}$ as the equivalent of three or more phase currents of a machine winding, even though a pair of phase windings aligned to the α- and the β-axis may not physically exist. Zero sequence components do not contribute to the air-gap field.

The two windings in Fig. 2(a) are electrically and magnetically independent if linearized magnetics are assumed. They exhibit identical dynamic behavior, provided they have the same winding geometries. Hence the β-axis winding is described by an equation similar to (3),

$$u_{s\beta} = r_s i_{s\beta} + l_s \frac{di_{s\beta}}{d\tau} + u_{e\beta}\,. \qquad (4)$$

The signal flow graph of the complete stator winding, Fig. 2(c), is derived from (3) and (4), using the scalar

winding currents i_α and i_β as state variables. The root locus plot in Fig. 2(d) shows that two real eigenvalues exist; they are both located at $-1/\tau_S$, provided the back emf is independent from the stator current. The eigenvalues underline the characteristics of the dynamic system as seen from the machine terminals: Two independent low-pass circuits, each being composed of a resistor and an inductor.

The definitions $\boldsymbol{u}_s = u_{sa} + j\, u_{sb}$ and $\boldsymbol{i}_s = i_{s\alpha} + j\, i_{s\beta}$ reflect the orientation of the two phase windings in space, permitting a complex notation of (3) and (4)

$$\boldsymbol{u}_s = r_s \boldsymbol{i}_s + l_s \frac{d\boldsymbol{i}_s}{d\tau} + \boldsymbol{u}_e . \qquad (5)$$

2.3 Rotating reference frame

It is expedient to describe the respective windings in the rotor and in the stator of an electric machine in a common reference frame. The angular orientation of such coordinate system may be either fixed to the stator, or considered rotating in synchronism with the machine rotor, or in synchronism with the revolving magnetic field. In the general case, the stator windings as well rotate with respect to the coordinate system.

The transformation of the stator winding displayed in Fig. 2(a) into a rotating coordinate system, having an angular velocity ω_k with respect to the stator, leaves the magnitudes of the space vector quantities in (5) unaffected; only their phase angles change. These get reduced by

$$\vartheta_k(\tau) = \int_0^\tau \omega_k d\tau + \vartheta_k(0), \quad (6)$$

if ω_k is counted positive in the direction of the revolving field. $\vartheta_k(0) = 0$ when the origin of the time scale is properly chosen.

Multiplying (5) by $exp(-j\vartheta_k)$ and observing $d\vartheta_k/d\tau = \omega_k$ from (6), we obtain the voltage equation of a three-phase stator winding in the general k-coordinate system in state space form

$$\frac{d\boldsymbol{i}_s^{(k)}}{d\tau} = -\left(\frac{1}{\tau_s} + j\omega_k \right) \boldsymbol{i}_s^{(k)} + \frac{1}{l_s} \left(\boldsymbol{u}_s^{(k)} - \boldsymbol{u}_e^{(k)} \right) \qquad (7)$$

Equation (7) is rearranged, and decomposed into its real and imaginary component

$$\tau_s \frac{di_{sd}}{d\tau} + i_{sd} = \omega_k \tau_s i_{sq} + \frac{1}{r_s}\left(u_{sd} - u_{ed} \right) \qquad (8a)$$

$$\tau_s \frac{di_{sq}}{d\tau} + i_{sq} = -\omega_k \tau_s i_{sd} + \frac{1}{r_s}\left(u_{sq} - u_{eq} \right), \qquad (8b)$$

from which the signal flow graph Fig. 3(a) is derived. It is different from the graph Fig. 2(c) in that a mutual cross-coupling between the two axes becomes apparent, the gain of which is proportional to the angular velocity ω_k of the k-coordinate system. The signal flow graph Fig. 2(c), in fact, results as the special case $\omega_k = 0$ of the graph Fig. 3(a).

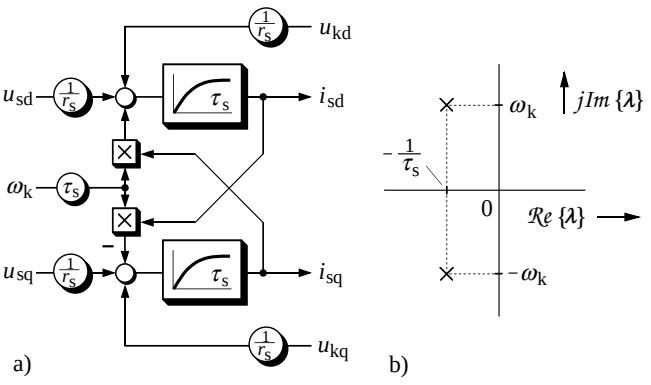

Fig. 3: Two-phase winding in rotating coordinates; a) signal flow diagram of space vector components, b) root locus showing a conjugate complex pole pair

Surprisingly, the eigenvalues of the stator winding, as seen from a rotating reference frame, differ from the ones in the stationary frame: Fig. 3(b) shows a pair of conjugate complex poles. They seem to attribute a different dynamic behavior to the winding, although only its mathematical description has changed.

2.4 Discussion of winding dynamics

The theory of dynamic systems associates two conjugate complex eigenvalues to an arrangement of two independent energy storage elements of different physical nature, having a coupling mechanism between them [5]. If energized, the storage elements exchange the energy periodically in the form of a harmonic oscillation. The resulting frequency is determined by the storage capacities of the two elements. This frequency is an inherent property of the system.

The two phase windings under consideration do represent two independent energy storage elements, but they are not coupled and hence an exchange of energy between them cannot occur. If observed from a rotating reference frame, the location in space of the total magnetic energy appears rotating. Taking the winding losses into consideration, this translates into damped oscillations in time of the transformed winding currents. The characteristic frequency ω_k is the angular velocity of the observation platform. This quantity can be arbitrarily chosen; it has no relationship with the eigenbehavior of the machine. Hence the observed oscillations are not a system property.

The winding analysis in a stationary reference frame (Section 2.2) correctly reveals two independent first-order systems. Changing to a synchronous reference frame introduces the angular frequency ω_k of the reference frame into the system equations. A second-order system now results, being characterized by the rotational frequency of the coordinate system. This is considered an unsatisfactory solution, and hence a different approach shall be followed. The continuous distribution in space of the magnetic energy is the basis of this approach.

3. Continuous Distributions

Sinusoidal distributions in space can be described by complex variables. The internal voltages, currents, and flux linkages of a polyphase winding exhibit such distributions, since the windings themselves are distributed in space. Their representation by complex space vectors, first proposed in 1959 by *Kovács* and *Rácz* [6], is meanwhile widely accepted [7]. On the other hand, nearly as many researchers prefer the matrix notation for the dynamic description of ac machines. Fundamental work was contributed by *Kron* [8], being based on the two-axes theory of *Park* [9]. A formal correspondence between both theories can be indeed observed by treating the scalar components of space vectors – their real and imaginary parts – as matrix elements and by considering the elements of the voltage equations of the stator and the rotor, according to *Kron*, as submatrices of the overall dynamic system.

The formal mathematical correspondence between the matrix approach and the space vector theory seems to support the notion of their physical equivalence. This is only true when considering the lumped parameter representation of a revolving field machine. The describing variables are then the external two-axis terminal voltages and currents. These variables are scalars. Against this, the internal distributions of current densities and flux densities, which give rise to a distributed force density along the airgap, and finally determine the locations of the magnetic energies in space, can be only described by complex state variables. The difference between the scalar and the complex approach was discussed in Section 2.1.

The following analysis takes advantage of the extended information contained in complex state variables.

3.1 Single polyphase winding

The state space equation (7) of the stator winding is written in complex form. The space vectors of voltages and currents in this equation represent continuous distributions in space. Computing the eigenvalues yields

$$det\left[\boldsymbol{\lambda} + \left(\frac{1}{\tau_\mathrm{s}} + \mathrm{j}\omega_\mathrm{k}\right)\right] = 0 \tag{9}$$

from which a single complex eigenvalue

$$\boldsymbol{\lambda}_1 = -\frac{1}{\tau_\mathrm{s}} - \mathrm{j}\omega_\mathrm{k} \tag{10}$$

is obtained. Note that a conjugate complex value does not exist. The result is obviously different from that was obtained previously from the eigenvalue analysis of (8). The presumption is raised at this point that the decomposition of a single first-order complex differential equation (7) into two real equations (8) of the same order is the cause of the inconsistency found in Section 2.4.

Further discussion is based on the graphic representation of the complex differential equation (7) by the signal flow diagram Fig. 4(a). The graph models the distributed two-axis winding in the stator by a complex first-order delay element, being excited by the stator voltage space vector $\boldsymbol{u}_\mathrm{s}$, and by a voltage vector $\boldsymbol{u}_\mathrm{e}$ which reflects the contribution of the rotor field.

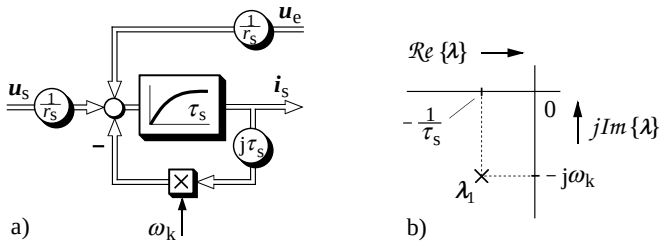

Fig. 4: Complex representation of a polyphase winding, a) fundamental structure, b) root locus showing a single complex pole

There is an internal feedback signal $-\mathrm{j}\omega_\mathrm{k}\,\tau_\mathrm{s}\,\boldsymbol{i}_\mathrm{s}$, which is inactive, $\omega_\mathrm{k} = 0$, if the chosen coordinate system is stationary with respect to the winding. As the coordinate system rotates at arbitrary positive angular velocity $\omega_\mathrm{k} \neq 0$, the internal feedback term contributes that particular component of the induced voltage which originates from the rotation of the winding conductors with respect to the reference frame. This is in accordance with *Faraday's* law. The negative sign of the feedback signal indicates, with respect to the ω_k-reference frame, a negative, or clockwise, rotation of the distributed magnetic field that links with this winding.

The root locus plot Fig. 4(b) confirms this interpretation and complies with the dynamic behavior of the winding as physically observable. A single complex pole charactarizes the system as a complex first-order delay, having the time constant $Re(\boldsymbol{\lambda}_1) = -1/\tau_\mathrm{s}$. The imaginary component $Im(\boldsymbol{\lambda}_1) = -\omega_\mathrm{k}$ indicates the rotational velocity of the winding with respect to the ω_k-reference frame. The velocity is negative (provided ω_k is positive), signaling a negative rotation of the winding as seen from the reference frame. The case of the reference frame being stationary with respect to the winding places the complex pole $\boldsymbol{\lambda}_1 = -1/\tau_\mathrm{s} + \mathrm{j}0$ on the real axis.

3.2 Stator and rotor windings

The dynamic analysis in its complex form is now extended to comprise both polyphase windings in the stator and in the rotor of an induction motor, which is the most proliferate type of ac machine used in variable speed drives.

The system equations in terms of complex space vector quantities are

$$\boldsymbol{u}_\mathrm{s} = r_\mathrm{s}\boldsymbol{i}_\mathrm{s} + \frac{d\boldsymbol{\psi}_\mathrm{s}}{d\tau} + \mathrm{j}\omega_\mathrm{k}\boldsymbol{\psi}_\mathrm{s} \tag{11a}$$

$$0 = r_\mathrm{r}\boldsymbol{i}_\mathrm{r} + \frac{d\boldsymbol{\psi}_\mathrm{r}}{d\tau} + \mathrm{j}(\omega_\mathrm{k} - \omega)\boldsymbol{\psi}_\mathrm{r}, \tag{11b}$$

and the flux linkage equations are

$$\boldsymbol{\psi}_\mathrm{s} = l_\mathrm{s}\boldsymbol{i}_\mathrm{s} + l_\mathrm{h}\boldsymbol{i}_\mathrm{r} \tag{12a}$$

$$\boldsymbol{\psi}_\mathrm{r} = l_\mathrm{h}\boldsymbol{i}_\mathrm{s} + l_\mathrm{r}\boldsymbol{i}_\mathrm{r}. \tag{12b}$$

The complex flux linkages of the stator and the rotor, $\boldsymbol{\psi}_s$ and $\boldsymbol{\psi}_r$, have been chosen as the state variables in these equations. This is an arbitrary decision. In fact, any two of the four space vectors $\boldsymbol{i}_s$, $\boldsymbol{\psi}_s$, $\boldsymbol{i}_r$, $\boldsymbol{\psi}_r$ serve this purpose. The selection depends on the particular problem at hand. Selecting the flux linkage vectors $\boldsymbol{\psi}_s$ and $\boldsymbol{\psi}_r$ as state variables yields the most straightforward dynamic structure.

The electromagnetic torque is proportional to the external product of two state variable space vectors, e. g. $|\boldsymbol{\psi}_s \times \boldsymbol{i}_s|$, forming the link to the dynamics of the mechanical system:

$$\tau_m \frac{d\omega}{d\tau} = |\boldsymbol{\psi}_s \times \boldsymbol{i}_s| - T_L , \qquad (13)$$

where τ_m is the normalized mechanical time constant, and T_L is the load torque. Note that ω_s and ω_r are the angular frequencies of the electrical quantities of the stator and the rotor, respectively; ω is the angular velocity of the rotor.

At least one, in the general case both machine windings see the common reference frame rotating, depending on the choice of ω_k in (11).

4. Dynamic Analysis

Using the general *k*-coordinate system, we obtain the system equations from (11) and (12) in the form

$$\tau_s' \frac{d\boldsymbol{\psi}_s}{d\tau} + \boldsymbol{\psi}_s = -j\omega_k \tau_s' \boldsymbol{\psi}_s + k_r \boldsymbol{\psi}_r + \tau_s' \boldsymbol{u}_s \qquad (14a)$$

$$\tau_r' \frac{d\boldsymbol{\psi}_r}{d\tau} + \boldsymbol{\psi}_r = -j(\omega_k - \omega) \tau_r' \boldsymbol{\psi}_r + k_s \boldsymbol{\psi}_s \qquad (14b)$$

where $\tau_s' = \sigma \tau_s$ and $\tau_r' = \sigma \tau_r$ are the transient time constants of the stator winding and the rotor winding, respectively, $k_s = l_h/l_s$ and $k_r = l_h/l_r$ are the magnetic coupling factors, and $\sigma = 1 - k_s k_r$ is the total leakage coefficient. The transient time constants replace τ_s in previous equations. This is owed to a magnetic cross-coupling between the state variables of the two winding systems. Such cross-coupling exists in cases where the machine is operated at forced stator voltage, and forced rotor voltage, including the special case $\boldsymbol{u}_r = 0$.

The eigenvalue analysis of (14) was carried out numerically to avoid tedious calculations. A stationary reference frame was used, $\omega_k = 0$, and the set of machine data given in the Appendix. The result is plotted in Fig. 5 with the mechanical speed ω as parameter.

The two single complex poles of the second-order system are located on the real axis at locked rotor, $\omega = 0$, indicating that the transient magnetic flux linkages of both the stator winding and the rotor winding are stationary with respect to the reference frame. The pole located close to the origin corresponds to a large time constant. It represents the field components that intersect the airgap and link with both windings in the stator and the rotor. The small airgap accounts for a large inductance, from which the large time constant results.

The pole on the left-hand side corresponds to a small time constant, representing the transient fields that extend tangentially in the airgap and cover a maximum distance of one pole pitch. The high magnetic resistance of this path accounts for a small inductance, and a small time constant results. Both time constants determine the rate of decay of the respective transient field components.

The two poles assume different positions when the machine rotates. Their respective real parts at nominal speed,

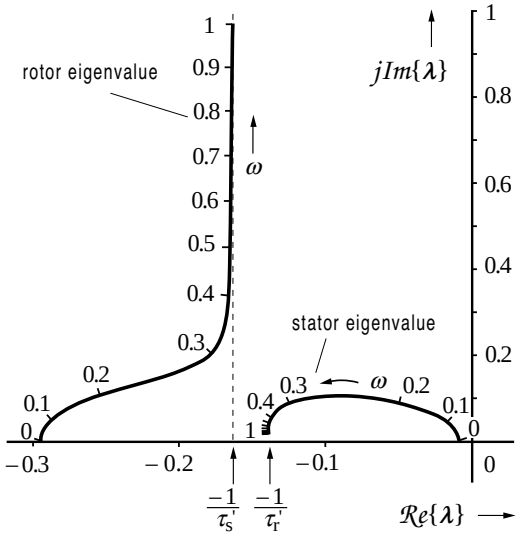

Fig. 5: Loci of the eigenvalues with the angular mechanical velocity ω as parameter, $\omega_k = 0$

$\omega = 1$, are determined by the inverse time constants of the system equations (14), $-1/\tau_s'$ and $-1/\tau_r'$. The imaginary parts indicate that the transient fields of both windings rotate in the average at the velocity of the associated winding: the stator field is almost stationary, and the rotor field exhibits nearly the same speed as the rotor itself. The small deviations between the field velocity and the velocity of the respective winding can be interpreted as a transient slip which results from a variable magnetic coupling between the windings. Since the two windings rotate with respect to each other, their magnetic coupling is not constant: the mutual inductance changes periodically in magnitude and sign with the frequency of the mechanical rotor speed. The transient slip is very small at nominal speed since the normalized corner frequencies of the first-order delays, $-1/\tau_s'$ of the stator and $-1/\tau_r'$ of the rotor, are around 0.15, hence much larger than the frequency of transient excitation, $\omega = 1$.

The root locus plot Fig. 5 shows that the dynamic interaction between the transient field components of the rotor and the stator reaches its maximum when the excitation, given by the rotor speed, comes close to the corner frequencies $-1/\tau_s'$ and $-1/\tau_r'$ of the first-order systems that characterize the two windings.

Note that the transient slip that occurs between a transient field component and the respective winding is determined by the eigenbehavior of the machine; the transient slip is different from the load dependent slip between the

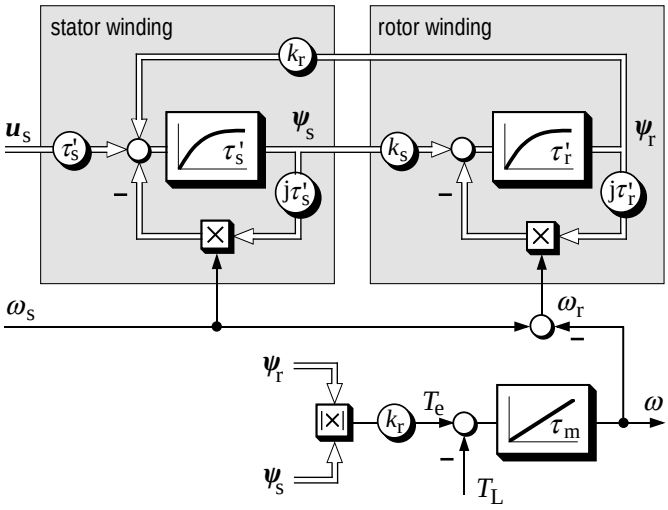

Fig. 6: Induction motor signal flow diagram; state variables: stator flux vector, rotor flux vector

fundamental steady-state field component and the rotor. The latter is proportional to the difference between the stator frequency and the mechanical speed, and hence is determined by the load condition.

5. Complex Signal Flow Graphs

The representation of polyphase windings by a first-order complex delay element and its visualization by a complex signal flow graph is now extended to describe the dynamic behavior of the entire machine. The resulting graphic structures depend on which pair of complex state variables is chosen from the possible set of the following four variables: $\boldsymbol{i}_s$, $\boldsymbol{\psi}_s$, $\boldsymbol{i}_r$, $\boldsymbol{\psi}_r$.

5.1 State variables: stator flux, rotor flux

The system equations in terms of the stator flux vector and the rotor flux vector have been previously derived, (14). Their representation in a complex signal flow graph Fig. 6 shows twice the fundamental structure Fig. 4(a) of a polyphase winding, representing the windings in the stator and the rotor, respectively.

It is now assumed for the following discussions that the coordinate system rotates in synchronism with the stator voltage space vector $\boldsymbol{u}_s$, hence $\omega_k = \omega_s$ in Fig. 6, and in all subsequent graphs. The vector $\boldsymbol{u}_s$ represents the feeding source voltage. The fundamental structure of the stator winding in Fig. 6 comprises a complex first-order delay having the transient time constant τ_s'. The multiplyingfactor ω_s in the complex feedback path and the negative sign at the subsequent summing point indicate that the winding rotates at the angular velocity $-\omega_s$ relatively to the reference frame.

The winding in the rotor exhibits a dynamic structure that is similar to that of the stator. It rotates at the angular velocity $-\omega_r = -(\omega_s - \omega)$ against the common reference frame, which follows from the parameters in the complex feedback path on the right-hand side of Fig. 6; the time constant of the rotor circuit is τ_r'.

The flux linkage vectors of the stator and the rotor act as the forcing functions on the respective opposite windings; the leakage fluxes are excluded from that magnetic intercoupling by virtue of the two coefficients k_s, $k_r < 1$. Equations (13) and (12b) serve to derive the electromagnetic torque

$T_e = k_r \cdot |\boldsymbol{\psi}_r \times \boldsymbol{\psi}_s|$ from the actual state variables. The result forms the input signal to the mechanical system in the lower portion of the graph.

As seen against the complexity of the dynamic structure of an induction motor, its signal flow diagram in complex form is fairly simple. It corresponds to the simplicity of the motor construction: there is one winding in the stator, and one winding in the rotor, and both are magnetically coupled with each other through the air-gap field. Exactly this is reflected by the two identical, mutually coupled fundamental structures in the signal flow graph.

5.2 State variables: stator current, rotor flux

5.2.1 Machine dynamics

Many drive control applications, especially those for high dynamic performance, include closed loop control of the stator currents. It is convenient in such case to consider the stator current vector $\boldsymbol{i}_s$ a state variable. If the rotor flux linkage vector is maintained as the second state variable, the system equations are

$$\tau_\sigma' \frac{d\boldsymbol{i}_s}{d\tau} + \boldsymbol{i}_s = -j\omega_k \tau_\sigma' \boldsymbol{i}_s + \frac{k_r}{r_\sigma}\left(\frac{1}{\tau_r} - j\,\omega\right)\boldsymbol{\psi}_r + \frac{1}{r_\sigma}\boldsymbol{u}_s \qquad (15a)$$

$$\tau_r \frac{d\boldsymbol{\psi}_r}{d\tau} + \boldsymbol{\psi}_r = -j(\omega_k - \omega)\tau_r \boldsymbol{\psi}_r + l_h \boldsymbol{i}_s, \qquad (15b)$$

which follows from (11) and (12). The coefficients in (15) are $\tau_\sigma' = \sigma l_s / r_\sigma$, and $r_\sigma = r_s + k_r^2\, r_r$. The graphical interpretation of (15) at $\omega_k = \omega_s$ is the signal flow diagram Fig. 7. This graph again exhibits two of the fundamental winding structures Fig. 4(a), representing the windings in the stator and the rotor, and their mutual magnetic coupling. The stator winding is characterized by the relatively small transient time constant τ_σ', which is determined by the leakage inductances and the winding resistances in the stator and the rotor. The rotor flux reacts with the stator through a forced voltage, predominantly determined by the term $-j\omega\tau_r\boldsymbol{\psi}_r$ unless the speed is very low.

The influence in the reverse direction, from the stator to the rotor, is of different nature: it is the stator mmf contribution to the magnetizing current of the rotor flux. The rotor field is produced by the sum of the stator and the rotor mmf; hence it is the large rotor time constant $\tau_r = l_r / r_r$ which characterizes the first-order delay in the rotor. The electromagnetic torque is computed from the chosen space vector state variables using (13) and (12).

It is interesting to note that the system Fig. 7 is characterized by two time constants that are different from those in Fig. 6, although the dynamic behavior of the system has obviously not changed. An explanation can be easily given for the special case of zero stator frequency operation, $\omega_s =$

0. Choosing the stationary reference frame, $\omega_k = 0$, eliminates both multipliers in the internal feedback loops of the rotor winding and the stator winding. The structure Fig. 6 then converts to a mere series connection of two first-order elements, arranged in a positive-feedback loop as shown in Fig. 8(a). The system has in fact reduced to the equivalent of a polyphase transformer, with all cross-couplings between the real and the imaginary components being zero. This locates the two single complex eigenvalues on the real axis.

Fig. 8(d) shows the locations of these poles. The eigenvalues $-1/\tau_s'$ and $-1/\tau_r'$ of the open-loop system are given by the time constants τ_s' and τ_r' of the first-order delay

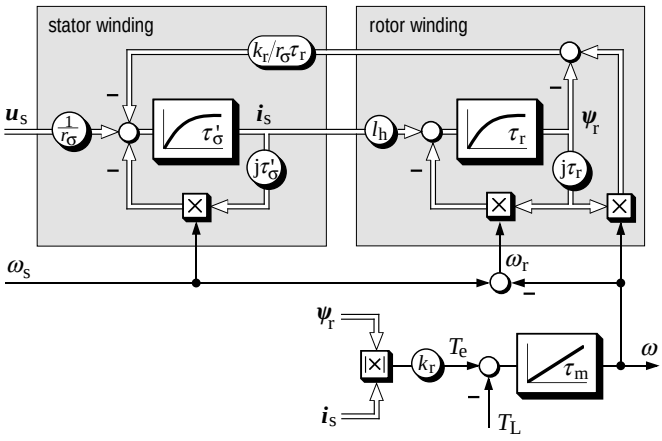

Fig. 7: Induction motor signal flow diagram; state variables: stator current vector, rotor flux vector

elements. The positive-feedback gain places the poles $\boldsymbol{\lambda}_1$ and $\boldsymbol{\lambda}_2$ of the closed-loop system at greater distance from each other. They correspond to the respective values at $\omega = 0$ in Fig .5.

Similarly, the signal flow diagram Fig. 7 converts to an identical structure at $\omega_s = \omega_k = 0$ as shown in Fig. 8(b). However, the time constants of the delay elements are now different; the open-loop poles are located at $-1/\tau_\sigma'$ and $-1/\tau_r$. It is apparent that the total gain $l_h\, k_r/r_\sigma\, \tau_r$ of the closed-loop system in Fig. 8(b) must be much smaller than in the previous case, since the open-loop poles are already in very close proximity to the closed-loop poles.

5.2.2 Rotor field orientation

A fast current control system is well suited to force the stator mmf distribution to any desired location and intensity in space, independent of the machine dynamics. The dynamic order then reduces, the system being characterized by a single complex equation

$$\tau_r \frac{d\boldsymbol{\psi}_r}{d\tau} + \boldsymbol{\psi}_r = -j\omega_r \tau_r \boldsymbol{\psi}_r + l_s \boldsymbol{i}_s, \qquad (16)$$

in which the stator current is the forcing function, determined by the reference signal of the current control loop.

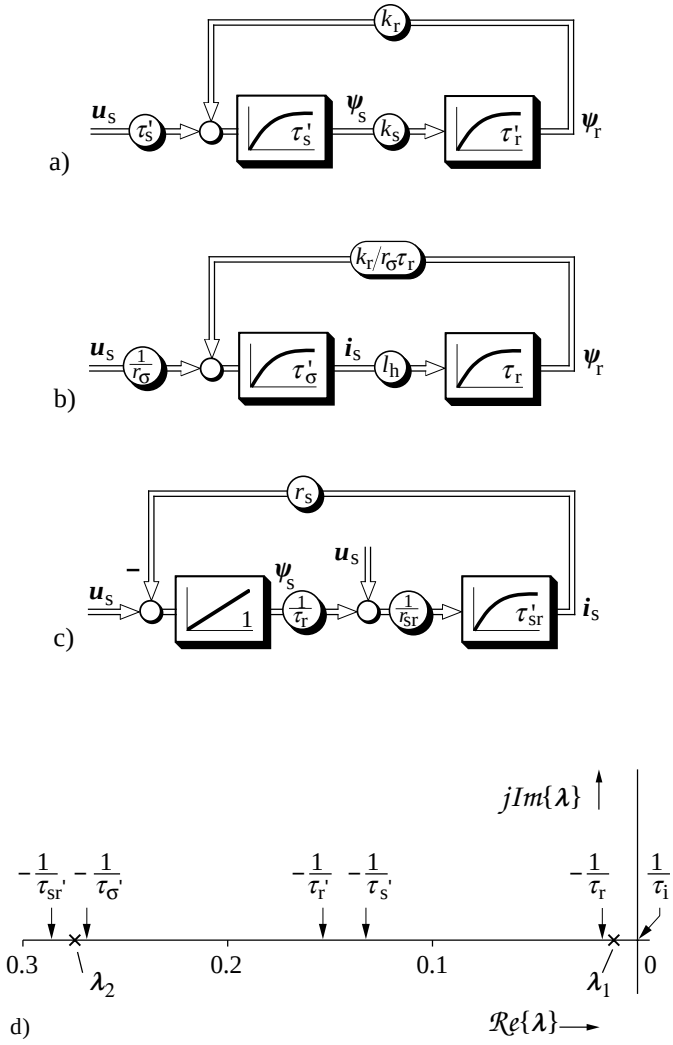

Fig. 8: Signal flow diagrams of the induction motor at $\omega = 0$ in a stationary reference frame: $\omega_k = 0$; The open loop time constants depend on the respective state variables: (a) stator flux and rotor flux, (b) stator current and rotor flux, (c) stator current and stator flux. d) shows the location of open-loop eigenvalues $1/\tau_x$ and complex closed-loop eigenvalues $\boldsymbol{\lambda}_n$ for the three combinations of state variables shown in (a) through (c). (The integrator time constant is located in the origin).

Equation (16) translates to the signal flow graph Fig. 9(a), which has a very simple structure.

The digital signal processing part of the drive control system is most frequently designed such that the space vector components are referred to in a *dq*-coordinate system, the real axis of which is aligned with the rotor flux vector. The imaginary rotor flux component ψ_{rq} is then zero by definition. The method is called control by rotor field orientation [7]; it requires the on-line identification of the rotor flux vector, using for instance a machine model or a state observer, since the rotor state variables cannot be directly measured in a squirrel cage machine.

Fig. 9(a) shows that the condition of field orientation is characterized by a zero output signal, and consequently by a zero input signal, of the imaginary channel of the first-order delay. Signals of zero magnitude are represented by

dotted lines in Fig. 11. A zero input signal is enforced observing the condition

$$\omega_r \tau_r \psi_{rd} = l_h i_{sq} \tag{17}$$

at the summing point. This can be directly read from the signal flow graph. The condition determines that value ω_r of the rotor frequency that is required to ensure field orientation. This value is established by operating the machine at stator frequency $\omega_s = \omega_r + \omega$, where the angular velocity ω of the rotor is a state variable which can be measured in a practical application.

Equation (17) is the condition for rotor field orientation; it enforces $\psi_r = \psi_{rd} + j0$. The condition renders the dotted signals in Fig. 9(a) zero, permitting to restructure the signal flow graph as shown in Fig. 9(b). Since ψ_{rd} is defined as zero, the rotor field is only represented by ψ_{rd}. Note that the space vector components ψ_{rd} and ψ_{rq}, and i_{sd} and i_{sq} as well, maintain the properties of space vectors since they represent sinusoidal distributions in space, or components thereof. This definition was developed in Section 2.1; it forms the basis of the dynamic representation of ac machines by complex state variables.

The method of rotor field orientation eliminates the undesired dynamic coupling between machine variables. The signal flow graph Fig. 9(b) shows that the *d*-current controls the rotor flux, and the *q*-current controls the torque. A dynamic interaction from i_{sd} to the torque is almost inhibited by the large time constant τ_r.

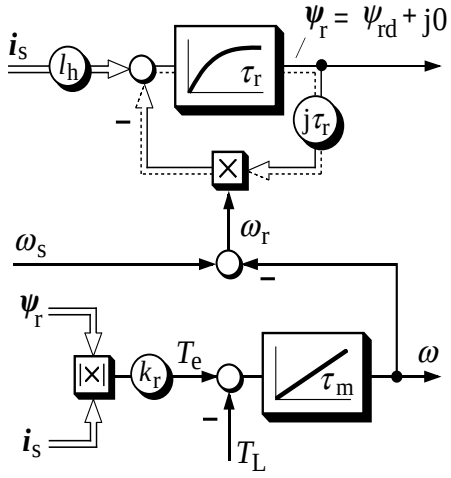

a)

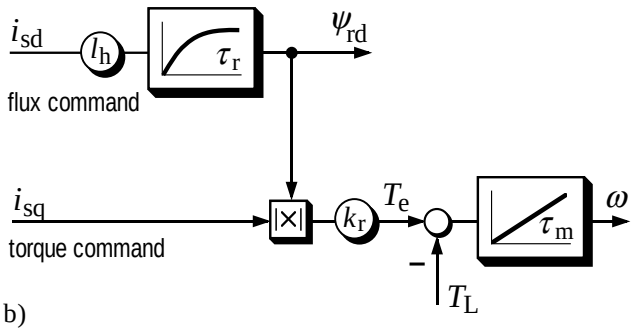

b)

Fig. 9: Induction motor at forced stator currents; a) complex signal flow graph, (the dotted lines represent signals of zero magnitude if field orientation is enforced), b) resulting structure at field orientation.

5.3 State variables: stator current, stator flux

If the drive control philosophy requires processing of the stator flux linkage signals, the machine dynamics are represented with preference in terms of the state variables ψ_s and i_s.

The system equations are derived from (11) and (12)

$$\frac{d\psi_s}{d\tau} = -j\omega_k \psi_s - r_s i_s + u_s \tag{18a}$$

$$\tau_{sr}' \frac{di_s}{d\tau} + i_s = -j(\omega_k - \omega)\tau_{sr}' i_s + \frac{1}{r_{sr}}\left(\frac{1}{\tau_r} - j\omega\right)\psi_s + \frac{1}{r_{sr}} u_s \tag{18b}$$

where $\tau_{sr}' = \sigma l_s / r_{sr}$ and $r_{sr} = r_s + l_s/l_r \cdot r_r$. The corresponding signal flow graph is shown in Fig. 10.

The stator flux vector in this graph is generated as the integral of $u_s - r_s i_s$, the normalized time constant of the integrator being unity. The internal feedback signal $-j\omega_s \psi_s$ associated to the stator winding is nonzero whenever the coordinate system rotates against this winding.

Curiously, the dynamic representation by the two stator state variables ψ_s and i_s, renders the stator current i_s the state variable describing the rotor winding. This is apparent from the ω_r-signal input to the fundamental structure on the right-hand side of Fig. 10. The signal, in fact, represents the angular velocity of the rotor against the reference frame.

There is a strong coupling from the stator flux to the stator current, expressed by the high value of the coefficient $1/r_{sr}$, being the inverse of the winding resistances. The significant contribution here is the rotor induced emf $-j\omega\psi_s$, unless the angular rotor velocity ω is very low. The strong physical affinity between ψ_s and i_s accounts for the stator voltage vector being an input to both winding systems, and for a small time constant τ_{sr}' in the rotor winding. Against this, the coupling from i_s to ψ_s in the return path is very weak, the normalized value of r_s being only a few percent.

For comparison, the system Fig. 10 is considered in the stationary reference frame, $\omega_k = 0$, at $\omega = 0$, from which structure Fig. 8(c) results. The open-loop time constants are now located at $-1/\tau_{sr}'$, and in the origin. Their location is shown in Fig. 8(d). Other than in the previous cases, the closed loop is now a negative-feedback system. Hence the closed-loop poles λ_1 and λ_2 are located at a shorter distance from each other than the open-loop poles.

6. Summary

A discusssion of the dynamics of ac machines using established system analysis techniques leaves scope for ambiguous interpretations. A pair of conjugate complex eigenvalues is assigned to a three-phase stator winding when described in a synchronous reference frame. This suggests that the winding as an independent dynamic system can execute self-sustained damped eigenoscillations. A

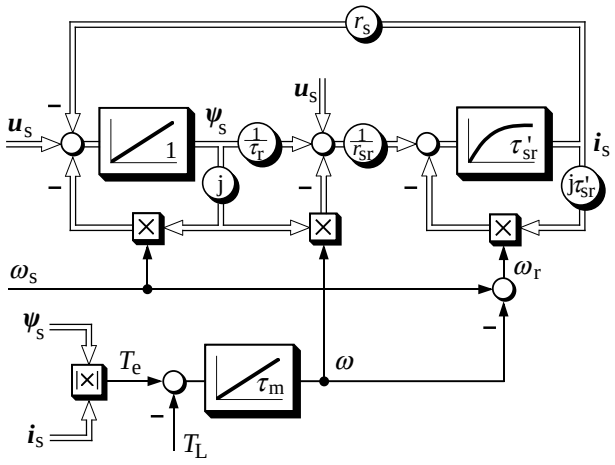

Fig. 10: Induction motor signal flow diagram; state variables: stator current vector, stator flux vector

clarification is reached when the analysis is based on complex space vectors as state variables instead of their scalar components. This makes eigenoscillations and the effects of rotational transformations distinguishable from each other.

The approach is an extension to the theory of dynamic systems. It leads to the definition of single complex eigenvalues that do not have conjugate values associated to them. Very favorably, the method permits a graphic representation of a polyphase machine winding by one complex first-order element. Twice this structure creates the complex signal flow graph of an induction motor. Complex signal flow graphs render the very involved and highly cross-coupled dynamic structure of ac machines intelligible by visual inspection.

7. Appendix

The following machine data were used for the computation of eigenvalues:

$l_s = 3.005, \quad r_s = 0.0446, \quad l_h = 2{,}89,$
$l_r = 3.13, \quad r_r = 0.054.$

8. References

1. D. Naunin, „Representation of the Dynamic Behavior of a Voltage-Fed Induction Motor by a Complex Second Order Delay (in German)", *Wiss. Berichte AEG-Telefunken, Vol. 42*, 1969, pp. 53-57.
2. P. L. Jansen, R. D. Lorenz, „A Physically Insightful Approach to the Design and Accuracy Assessment of Flux Observers for Field Oriented Induction Machine Drives", Proc. IEEE IAS Annual Meeting, Houston/Tx, 1992, pp. 570-577.
3. H. Bühler, „Introduction to the Theory of Controlled Electrical Drives" (in German), *Birkhäuser, Basel*, 1977.
4. P. K. Kovács, „Transient Phenomena in Electrical Machines", *Elsevier Science Publishers, Amsterdam*, 1984.
5. K. Ogata, „State Space Analysis of Control Systems", *Prentice Hall Inc., Englewood Cliff, NJ.*, 1967.
6. P. K. Kovács and I Rácz, „Transient Phenomena in Electrical Machines" (in German), *Verlag der Ungarischen Akademie der Wissenschaften*, Budapest, 1959.